

Reversible Shuttle Action upon Dehydration and Rehydration Processes in Cationic Coordinatively-Bonded (4,4) Square-Grid Nets Threaded by Supramolecular Bonded Anions, $\{[\text{Cu}^{\text{II}}(4,4'\text{-bpy})_2(\text{H}_2\text{O})][\text{Cu}^{\text{II}}(2\text{-pySO}_3)_3](\text{NO}_3)\} \cdot \text{H}_2\text{O}$

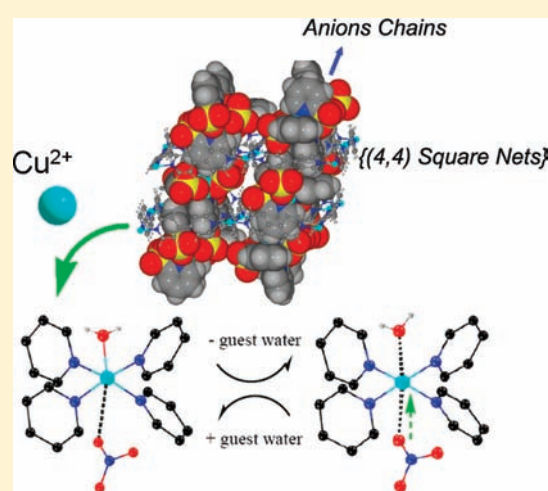
Yi-Min Jiang,[†] Zheng Yin,[†] Kun-Huan He,[†] Ming-Hua Zeng,^{*,†} and Mohamedally Kurmoo^{*,†}

[†]Key Laboratory for the Chemistry and Molecular Engineering of Medicinal Resources (Ministry of Education), School of Chemistry and Chemical Engineering of Guangxi Normal University, Guilin 541004, P. R. China

^{*}Laboratoire DECOMET, CNRS-UMR 7177, Université de Strasbourg, 4 rue Blaise Pascal, CS 90032, 67081 Strasbourg, France

S Supporting Information

ABSTRACT: $\{[\text{Cu}^{\text{II}}(4,4'\text{-bpy})_2(\text{H}_2\text{O})][\text{Cu}^{\text{II}}(2\text{-pySO}_3)_3](\text{NO}_3)\} \cdot \text{H}_2\text{O}$, obtained serendipitously by the reaction of the constituents in water, consists of parallel coordinatively bonded cationic (4,4) corrugated square-grids polymer of $\{[\text{Cu}^{\text{II}}(4,4'\text{-bpy})_2(\text{H}_2\text{O})]^{2+}\}_n$ threaded by π - π and H-bonded supramolecular chains of $[\text{Cu}^{\text{II}}(2\text{-pySO}_3)_3]^-$ through the open squares. A single-crystal to single-crystal transformation takes place upon removal of the noncoordinated water by controlled heating. The resulting structure exhibits a rearrangement of the coordination of the copper atoms in the grids, where the Cu–H₂O bond is elongated from 2.250(3) to 2.628(3) Å while the Cu–NO₃ is shortened from 3.122(3) to 2.796(1) Å. This process is reversible as demonstrated by the single crystal structure after rehydration with corresponding bond distances of 2.224(3) and 3.152(3) Å. Such a cooperative effect may be associated with the Jahn–Teller distortion of the copper(II) ion accompanying the shuttle action of the hydrogen-bonded water and nitrate moiety.



INTRODUCTION

Coordination polymers are of increasing interest due to their fascinating structural topologies and potential applications as functional materials.¹ Among different types of net-based coordination polymers, those displaying an open structure have received more attention due to their potential application as hydrogen storage.² When the open space is occupied by molecular guests, understanding the existing interactions between the host and these guests is expected to provide useful relationships between structure and gas sorption properties.³ Utilizing multi-component host–guest systems to prepare precisely controlled multidimensional motifs via molecular recognition remains an interesting challenge.⁴ It is well-established that weak bonding interactions between entities, such as hydrogen-bonding and π - π stacking, are important supramolecular forces, which can be used to govern the process of molecular recognition and self-assembly.^{4–6} Though predictable in rare cases, in general serendipity results in the most stable structures where these interactions play an important role.¹ As such it is not surprising that very few aromatic π -interactions structure-directing threading networks have been reported.⁷ On the other hand, copper(II) is the

classical example for the Jahn–Teller effect (JTE), observed in the distorted stereochemistry of its complexes. Therefore, copper can display long bonds with oxygen and nitrogen donor ligands as well as being stable in coordination numbers of 4 to 6 while adopting highly distorted and nonsymmetric geometries. It is well documented that the distortion can be dynamic JTE, cooperative JTE, or JT switch.⁸ Such a variable stereochemistry process is, however, seldom observable in the literature of metal–organic frameworks,⁹ especially through single-crystal to single-crystal X-ray diffraction studies because the drastic structural changes during the process readily cause loss of crystallinity.^{10,11}

Here we report the crystallographic observation of a reversible shuttle action of H₂O and NO₃[−] by single-crystal to single-crystal upon partial dehydration/rehydration of a system, $\{[\text{Cu}(4,4'\text{-bpy})_2(\text{H}_2\text{O})][\text{Cu}(2\text{-pySO}_3)_3](\text{NO}_3)\} \cdot \text{H}_2\text{O}$ (1) (bpy = bipyridine; 2-pySO₃ = 2-pyridine-sulfonate), consisting of stable coordinatively bonded (4,4) square-grids cationic layers

Received: October 4, 2010

Published: February 24, 2011

Table 1. Crystal Data and Structure Refinements for **1**, **2**, and **1'**

	1	2	1'
formula	C ₃₅ H ₃₂ Cu ₂	C ₃₅ H ₃₀ Cu ₂	C ₃₅ H ₃₂ Cu ₂
	N ₈ O ₁₄ S ₃	N ₈ O ₁₃ S ₃	N ₈ O ₁₄ S ₃
formula wt	1011.95	993.93	1011.95
temp/K	291(2)	173(2)	291(2)
cryst syt	monoclinic	monoclinic	monoclinic
space group	<i>P</i> ₂ ₁ / <i>c</i>	<i>P</i> ₂ ₁ / <i>c</i>	<i>P</i> ₂ ₁ / <i>c</i>
<i>a</i> /Å	14.816(1)	14.631(6)	14.734(5)
<i>b</i> /Å	15.478(1)	15.371(6)	15.427(6)
<i>c</i> /Å	17.719(2)	17.709(7)	17.592(6)
β /deg	99.877(1)	98.187(7)	99.584(7)
<i>V</i> /Å ³	4003.4(6)	3942(3)	3943(2)
<i>Z</i>	4	4	4
<i>D_c</i> /g/cm ³	1.679	1.675	1.705
μ /mm ⁻¹	1.298	1.315	1.318
no. of reflns collected	26157	31288	17531
no. of indep reflns	7432	7301	7287
<i>R</i> _{int}	0.0556	0.1180	0.0432
goodness of fit	1.018	1.188	1.033
<i>R</i> ₁ ^a [<i>I</i> > 2 σ (<i>I</i>)]	0.0459	0.1279	0.0418
<i>wR</i> ₂ ^a (all data)	0.1230	0.3101	0.1257

$$^a R_1 = \frac{\sum ||F_o| - |F_c||}{\sum |F_o|}, wR_2 = \left[\frac{\sum w(F_o^2 - F_c^2)^2}{\sum w(F_o^2)^2} \right]^{1/2}$$

threaded through the open spaces by one-dimensional chains of supramolecularly bonded anions.

EXPERIMENTAL SECTION

Synthesis. A mixture of Cu(NO₃)₂·3H₂O (0.121 g, 0.5 mmol), NaOH (0.04 g, 1.0 mmol), pyridine-2-sulfonate (0.158 g, 1.0 mmol), and H₂O (10.0 mL) was stirred and refluxed at 333 K for 1 h. 4,4'-bipy (0.078 g, 0.5 mmol) in MeOH (10 mL) was then added and the reaction continued for another 2 h. After the reaction was slowly cooled to room temperature, the blue block crystals of {[Cu(4,4'-bpy)₂(H₂O)]₂[Cu(2-pySO₃)₃](NO₃)}·H₂O (**1**) were collected by filtration, washed with water, and dried at ambient temperature. Yield: 40% (based on Cu). Elemental analyses (%). Calcd for **1** (C₃₅H₃₂Cu₂N₈O₁₄S₃): C, 41.29; H, 3.06; N, 11.29; S, 9.56. Found: C, 41.54; H, 3.19; N, 11.07; S, 9.51. IR (KBr, cm⁻¹): 3448(s), 3091(m), 1611(m), 1536(w), 1497(w), 1424(m), 1384(s), 1324(m), 1291(m), 1272(m), 1225(m), 1196(s), 1164(s), 1098(m), 1073(m), 1023(s), 1014(m), 843(w), 828(w), 739(m), 645(m), 630(m). The partially desolvated phase [Cu(4,4'-bpy)₂(H₂O)]₂[Cu(2-pySO₃)₃](NO₃) (**2**) was obtained by heating single crystals of **1** at 453 K for 1 h. The resolvated phase **1'** was generated by the exposure of **2** to air at room temperature.

Crystal and Structure Refinement Parameters for **1, **2**, and **1'**.** Diffraction intensities of all compounds were collected on a Bruker Apex CCD area-detector diffractometer (Mo K α , λ = 0.71073 Å). Absorption corrections were applied by using multiscan program SADABS.¹² The structures were solved by direct methods and refined with a full-matrix least-squares technique using the SHELXTL program package.¹³ All non-hydrogen atoms were refined with anisotropic displacement parameters. The organic hydrogen atoms were generated geometrically (C–H 0.96 Å). The crystal data and structure

Table 2. Selected Bond Distances and Bond Angles for **1**, **2** and **1'**^a

	1	2	1'
Cu(1)–N(1)	2.076(3)	2.075(11)	2.063(3)
Cu(1)–N(2)	2.011(3)	2.020(11)	2.008(3)
Cu(1)–N(3)	2.000(4)	2.032(10)	2.002(3)
Cu(1)–O(1)	2.339(3)	2.335(10)	2.340(3)
Cu(1)–O(6)	2.018(3)	2.015(10)	2.015(3)
Cu(1)–O(7)	2.257(3)	2.274(10)	2.258(3)
Cu(2)–N(4)	2.025(3)	2.013(11)	2.010(3)
Cu(2)–N(5)	2.017(3)	2.002(10)	2.012(3)
Cu(2)–N(6)	2.028(3)	2.019(11)	2.026(3)
Cu(2)–N(7a)	2.036(3)	2.008(11)	2.020(3)
Cu(2)–O(1w)	2.250(3)	2.628(26)	2.224(3)
Cu2···O10	3.122(3)	2.796(12)	3.152(3)
N(3)–Cu(1)–N(2)	163.7(1)	163.6(4)	163.0(1)
N(1)–Cu(1)–O(1)	79.6(1)	80.2(4)	79.5(1)
N(3)–Cu(1)–O(7)	81.8(1)	81.0(4)	81.4(1)
N(1)–Cu(1)–O(7)	96.5(1)	94.7(4)	96.5(1)
O(6)–Cu(1)–O(1)	88.3(1)	89.9(4)	88.6(1)
N(5)–Cu(2)–N(6)	89.5(1)	90.0(4)	89.7(1)
N(4)–Cu(2)–N(6)	89.6(1)	89.9(4)	89.2(1)
N(5)–Cu(2)–N(7a)	90.2(1)	90.8(4)	89.8(1)
N(5)–Cu(2)–O(1w)	91.5(1)		92.0(1)
N(4)–Cu(2)–O(1w)	97.1(1)		97.6(1)

^a Symmetry Codes: (a) $-x, y + 1/2, -z + 1/2$.

refinement results for these compounds are listed in Table 1. Selected bond distances and bond angles are listed in Table 2. Hydrogen bonds for **1**, **2**, and **1'** are listed in Table S1. CCDC No. 795219, 795220, 795221, for compound **1**, **2**, and **1'**, respectively, contain the supplementary crystallographic data for this paper. These data can be obtained free of charge via www.ccdc.cam.ac.uk/conts/retrieving.html (or from the Cambridge Crystallographic Centre, 12 Union Road, Cambridge CB21EZ, UK; Fax: (+44)1223-336-033; or e-mail: deposit@ccdc.cam.ac.uk).

RESULTS AND DISCUSSION

X-ray structural analysis of **1** showed that there are two distinct crystallographically unique copper atoms per asymmetric unit (Figure 1), which have different coordination environments and belong to two independent nets, a cationic coordinatively bonded (4,4) square grid {[Cu₂(4,4'-bpy)₂(H₂O)]²⁺}_n and an anionic supramolecularly bonded chain of [Cu1(2-pySO₃)₃]⁻. The Cu1 of the anion adopts a distorted N₃O₃ octahedral coordination environment surrounded by three pyridine nitrogen atoms (2.000(3)–2.076(4) Å) and three sulfonate oxygen atoms (2.018(3)–2.258(3) Å) (Figure 1a). The three 2-pySO₃ ligands adopt chelating mode and create six-coordination at the Cu1 ion, forming the 0-D complex anion, [Cu1(2-pySO₃)₃]⁻ which has the dimension 6.76 × 8.29 × 9.78 Å. The Cu2 of the cationic component (Figure 1b), {[Cu₂(4,4'-bpy)₂(H₂O)]²⁺}_n, adopts a square pyramidal geometry with four equatorial nitrogen atoms from four different bpy ligands (Cu2–N = 2.017(3)–2.036(3) Å) and the axial site is filled by a coordinated water molecule (Cu2–O1w = 2.250(3) Å). The Cu^{II} centers are

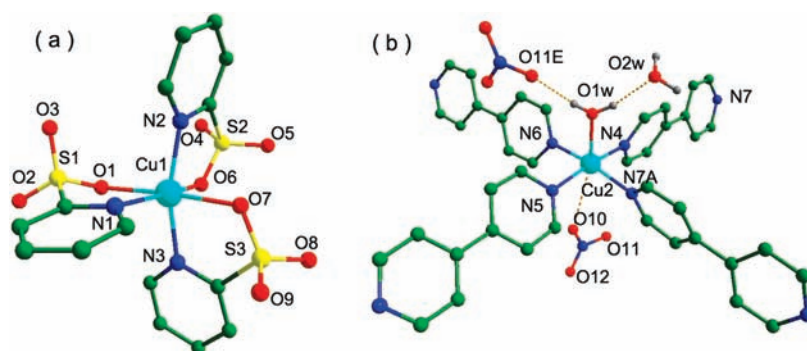


Figure 1. (a) Coordination geometries of the metal ions in the anionic complex, $[\text{Cu}(2\text{-pySO}_3)_3]^-$; (b) coordination geometries of the metal ions in the cationic component, $\{[\text{Cu}(4,4'\text{-bpy})_2(\text{H}_2\text{O})]^{2+}\}_n$. The weak coordinated NO_3^- and guest water molecule are included (symmetry codes: (a) $-x, y + 1/2, -z + 1/2$; (b) $x, -y + 3/2, z + 1/2$). Some hydrogen atoms have been omitted for clarity.

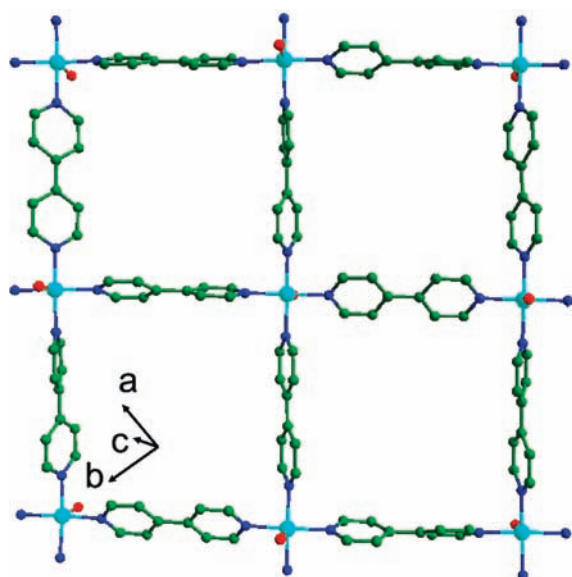


Figure 2. View of the square grids of $\{[\text{Cu}(4,4'\text{-bpy})_2(\text{H}_2\text{O})]^{2+}\}$ along the c -axis of **1**. The anions, $[\text{Cu}(2\text{-pySO}_3)_3]^-$, NO_3^- , and guest water molecules are not shown. Hydrogen atoms have been omitted for clarity.

bridged by 4,4'-bpy ligands to form a 2D sheet having square grids with corner angles of ca. 89 and 91°. The dihedral angle between the pyridyl rings of the bpy ligands in the two nonequivalent sides of the square grids is 0° and 29°, respectively.

Adjacent grids are parallel and stack on each other with an ABAB motif and a separation of 8.86 Å, therefore generating rectangular channels 6.78 × 6.78 Å (taking account of the van der Waals radii for constituent atoms) along the c -axis (Figure 2). More interesting, the NO_3^- anions act as linker between neighboring 2D sheets through weak bonding interaction with Cu(II) atoms ($\text{Cu}2 \cdots \text{O}10 = 3.122(3)$ Å) as well as hydrogen-bonding interaction with the coordinated water molecule of neighboring 2D sheets ($\text{O}1w \cdots \text{O}11 = 2.78$ Å; $\text{O}1w \cdots \text{H} \cdots \text{O}11 = 174.2^\circ$).

A fascinating and peculiar feature of **1** is the complex anions. Adjacent $[\text{Cu}1(2\text{-pySO}_3)_3]^-$ form 1D anionic chains along the c axis through π - π stacking and hydrogen bonds (Figure 3a). The T-shape anions are positioned to favor overlap between the aromatic rings as flanking arms. The pyridyl rings of the anions, embedded in the host square grids, are parallel to each other and face-to-face with center-to-center distances of 3.51 and 3.74 Å,

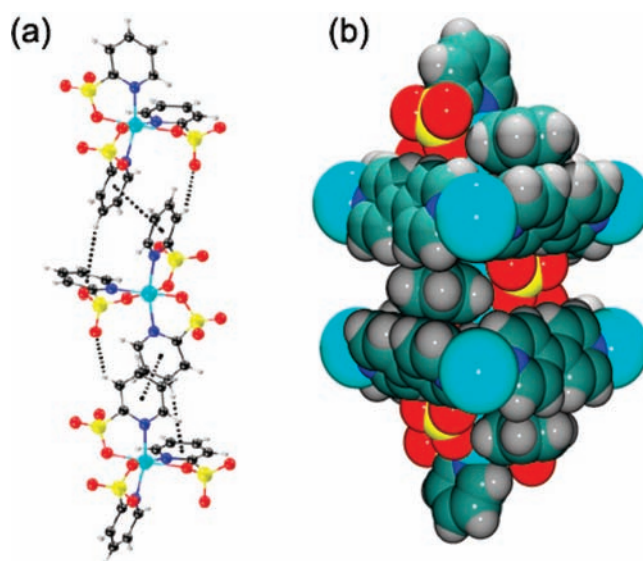


Figure 3. (a) The π - π stacking chain formed between anionic $[\text{Cu}(2\text{-pySO}_3)_3]^-$ units and its C-H \cdots O interactions are included; (b) space-filling view of the rod-to-ring interaction.

respectively, indicating significant π - π interaction. A C-H \cdots O hydrogen bonding ($\text{C}14 \cdots \text{O}3 = 3.09$ Å) and a moderate C-H \cdots π interaction with $\text{H}(8) \cdots$ centroid distances of 2.90 Å which interlink the adjacent complex anions also exist between inserted pyridyl and noninserted pyridyl ring. The use of a complex anion for a coordination network is very unusual.¹⁴ In this case the arrangement of the anion chain prevents the formation of an interpenetrated grid. Scheme 1 presents the way the supramolecular chains thread into the square grids and every square grid is restricted to a particular segment by the flanking rings, which extend the architectures to 3D threading networks (Figure 3b, Figure 4). This type of 3D threading structure constructed by two different motifs is rare, especially for π - π stacking motifs. The compound $[\text{Cu}_2(\text{bpa})_2(\text{phen})_2(\text{H}_2\text{O})]_2 \cdot 2\text{H}_2\text{O}$ [bpa = biphenyl-4,4'-dicarboxylate, phen = 1,10-phenanthroline] may be regarded as containing tendencies similar to the phen ligands providing self-assembly via π - π interaction to form 3D interlocking network.¹⁵

A detailed view of the rod-to-ring threading interaction is shown in Figure 3a. The sulfonate groups are expected to be

Scheme 1. 1D Chains Thread into Square Grids of 2D Layers, Extending a 3D Architecture

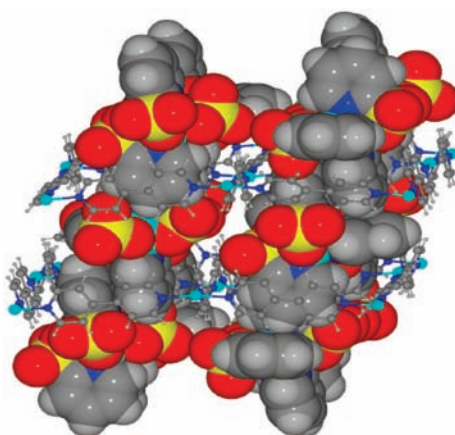
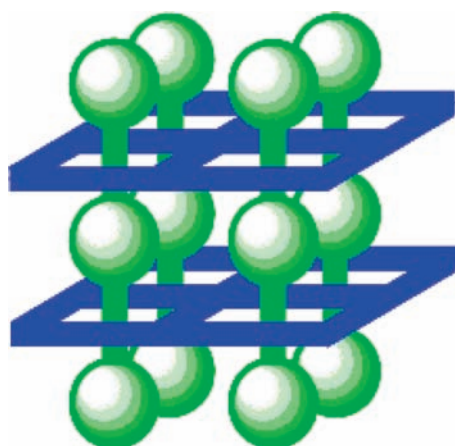


Figure 4. View of the 3D net constructed from square-grids and its complementary π - π stacking anionic chains.

excellent hydrogen bond acceptors. There are many C–H \cdots O contacts involving the aromatic C–H groups of square grids and the oxygen atoms of sulfonate group of the anion. The C \cdots O distances and the C–H \cdots O angles are in the range 3.14–3.45 Å and 121.8–169.5°, respectively. This indicates that the structure is strongly determined by H-bonding between the grids and its complementary anions as well as between anionic complexes themselves. The guest water molecule is also H-bonded to the oxygen atoms of the sulfonate group (O2w \cdots O = 2.83–2.87 Å).

Determination of the structure of **2** revealed a change of the geometrical parameters of copper atoms in the cationic component, in response to the guest water molecules removal (Figure 5). The apical coordinated water molecules are displaced from the copper atom (Cu–O(H₂O) from 2.250(3) to 2.628(26) Å), while the nitrate moves closer to the copper atom (Cu–O(NO₃) from 3.122(3) to 2.796(12) Å) but retains its weak interaction with the moving water molecule (from O1w \cdots O11 = 2.78 Å; O1w–H \cdots O11 = 174.2° to 2.81 Å and 176.7°, respectively) from the adjacent layer. Such kind of copper–oxygen distance is considerably long and beyond the range of coordination interaction, it is however less than the sum of van der Waals radii of copper and oxygen (3.55 Å).¹⁶ Upon

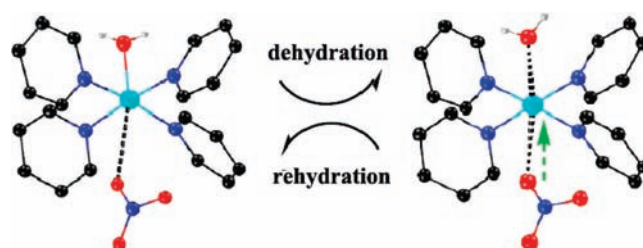


Figure 5. Coordination geometries of square grids in **1** undergo a reversible change upon removal and reload of guest water molecules.

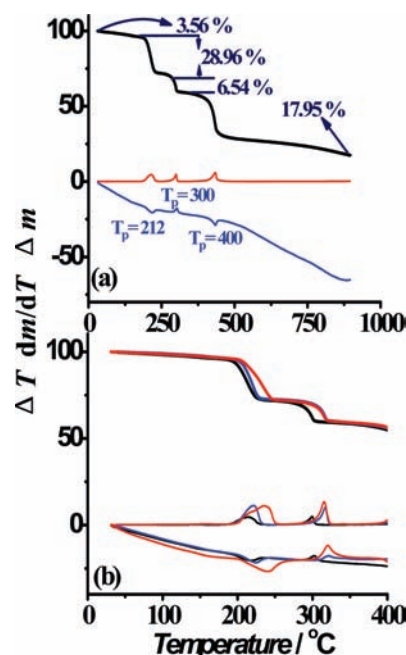


Figure 6. (a) TG, DTG, DTA curves for powdered samples of **1** (heating rate: 5 °C/min, N₂ atmosphere; T_p = peak temperature); (b) rate dependent reversibility in the TG, DTG, DTA curves during the dehydration processes at the following heating rates: 5 °C/min (black line), 10 °C/min (blue line), 15 °C/min (red line); N₂ atmosphere.

exposure of **2** to air at room temperature, it reverses to the rehydrated phase **1'**. X-ray structural analysis reveals that the weak coordinated water molecules chemically bind to copper atoms and the nitrate ions go back into their former positions. The apical-ligand-change might be due to the loss of restrictedness from H-bonding associated guest water molecules. This shuttle motion action of the two entities, H₂O and NO₃[−] as a pair, between the sheets may be helped by the subtle stabilization energies of the two Jahn–Teller geometries in the two states.⁸

The thermal stability of **1** was examined by TGA under N₂. Four mass steps over the temperature range 25–900 °C are observed in the TG curve that were accompanied with endothermic events in the DTA curve (Figure 6a). The mass loss in the first step of 3.22% is in good agreement with that calculated for the removal of both the coordination and guest water molecules, 3.56%. The second experimental mass loss of 28.96% (ca. 30.83%) is in rough agreement with the loss of two 4,4'-bipy as might be due to the presence of high fold rod-torcing threading C–H \cdots O. Hence one can assume that the thermal reaction began with decomposition of the square grids coordination polymer $\{[\text{Cu}(4,4'\text{-bpy})_2(\text{H}_2\text{O})]^{2+}\}_n$. The third

TG step with a mass loss of 6.54% is in reasonable agreement with that calculated for the removal of an additional 2/5 part of a 2-pySO_3^- anion (ca. 6.33%). In the temperature range 400–900 °C, the pyrolysis of the remaining parts with the final mass of 17.95%, which is higher than the deposition of CuO (ca. 15.72%) suggesting some sulfide may be present. Heating-rate-dependent TGA measurements for 10 and 15 K/min were also performed (Figure 6b). It is noted that removal rates of the coordination and guest molecules were dependent on the heating rate and the resolution can be improved when lower heating rate is used. Investigations of the thermal behavior using different methods would give more insight into the chemical reactivity and mechanisms of the thermal reactions of a coordination polymer.¹⁷

CONCLUSION

In conclusion, we have presented the synthesis and characterization of a fascinating coordination system involving coordinatively bonded (4,4) cationic square-grids threaded by a chain of supramolecularly bonded anions through π – π and hydrogen-bonding interactions. Reversible single-crystal to single-crystal transformation is observed upon dehydration and rehydration processes with an accompanied motion of coordinated water out of the sphere of coordination while the nonbonded NO_3 enters on the opposite side. This shuttle motion action of the two entities, H_2O and NO_3 as a pair, between the sheets may be helped by the subtle stabilization energies of the two Jahn–Teller geometries in the two states.

ASSOCIATED CONTENT

S Supporting Information. Hydrogen bonds table, X-ray crystallographic files in CIF format, conductivity measurement, and figure of electrical conductivity measurements. This material is available free of charge via the Internet at <http://pubs.acs.org>.

AUTHOR INFORMATION

Corresponding Author

*E-mail: znh@mailbox.gxnu.edu.cn (M.-H.Z.), kurmoo@unistra.fr (M.K.).

ACKNOWLEDGMENT

This work was supported by NSFC (91022015), GXSCF (2010GXNSFF013001, 0832001Z, 2010GXNSFD013017), and the Program for New Century Excellent Talents in University of the Ministry of Education China and GuangXi Province (NCET-07-217, 2006201). M.K. is funded by the CNRS (France).

REFERENCES

- (1) (a) Janiak, C. *Dalton Trans.* **2003**, 2781. (b) Kitagawa, S.; Kitaura, R.; Noro, S. *Angew. Chem., Int. Ed.* **2004**, *43*, 2334.
- (2) (a) Yaghi, O. M.; Li, Q.-W. *MRS Bull.* **2009**, *34*, 682. (b) Murray, L. J.; Dinca, M.; Long, J. R. *Chem. Soc. Rev.* **2009**, *38*, 1294. (c) Tranchemontagne, D. J.; Mendoza-Cortés, J. L.; O'Keeffe, M.; Yaghi, O. M. *Chem. Soc. Rev.* **2009**, *38*, 1257.
- (3) Kitagawa, S.; Matsuda, R. *Coord. Chem. Rev.* **2007**, *251*, 2490.
- (4) (a) Beatty, A. M. *Coord. Chem. Rev.* **2003**, *246*, 131. (b) Kepert, C. J. *Chem. Commun.* **2006**, 695.
- (5) (a) Ye, B.-H.; Tong, M.-L.; Chen, X.-M. *Coord. Chem. Rev.* **2005**, *249*, 545. (b) Janiak, C. *J. Chem. Soc., Dalton Trans.* **2000**, 3885.

- (6) (a) Zheng, S.-L.; Zhang, J.-P.; Wong, W.-T.; Chen, X.-M. *J. Am. Chem. Soc.* **2003**, *125*, 6882. (b) Long, L.-S.; Wu, Y.-R.; Huang, R.-B.; Zheng, L.-S. *Inorg. Chem.* **2004**, *43*, 3798. (c) Zeng, M.-H.; Zhou, Y.-L.; Zhang, W.-X.; Du, M.; Sun, H.-L. *Cryst. Growth Des.* **2010**, *10*, 20. (d) Chen, Q.; Zeng, M.-H.; Zhou, Y.-L.; Zou, H.-H.; Kurmoo, M. *Chem. Mater.* **2010**, *22*, 2114.
- (7) (a) Batten, S. R.; Robson, R. *Angew. Chem., Int. Ed.* **1998**, *37*, 1460. (b) Batten, S. R.; Neville, S. M.; Turner, D. R. The Royal Society of Chemistry: London, 2009; pp 273–372. (c) Zeng, M.-H.; Zhang, W.-X.; Sun, X.-Z.; Chen, X.-M. *Angew. Chem., Int. Ed.* **2005**, *44*, 3079.
- (8) Murphy, B.; Hathaway, B. *Coord. Chem. Rev.* **2003**, *243*, 237.
- (9) Kawano, M.; Fujita, M. *Coord. Chem. Rev.* **2007**, *251*, 2592.
- (10) (a) Takaoka, K.; Kawano, M.; Tominaga, M.; Fujita, M. *Angew. Chem., Int. Ed.* **2005**, *44*, 2151. (b) Chen, C.-L.; Goforth, A. M.; Smith, M. D.; Su, C.-Y.; zur Loye, H.-C. *Angew. Chem., Int. Ed.* **2005**, *44*, 6673.
- (11) (a) Zeng, M.-H.; Feng, X.-L.; Zhang, W.-X.; Chen, X.-M. *Dalton Trans.* **2006**, S294. (b) Zeng, M.-H.; Hu, S.; Chen, Q.; Xie, G.; Shuai, Q.; Gao, S.-L.; Tang, L.-Y. *Inorg. Chem.* **2009**, *48*, 7070.
- (12) Sheldrick, G. M. *SADABS 2.05*; University Göttingen: Göttingen, Germany, 2002.
- (13) (a) *SHELXTL 6.12*; Bruker Analytical Instrumentation: Madison, WI, 2000. (b) Spek, A. L. *J. Appl. Crystallogr.* **2003**, *36*, 7.
- (14) (a) May, L. J.; Shimizu, G. K. H. *Chem. Commun.* **2005**, 1270. (b) Han, Z.-B.; Zhang, G.-X.; Zeng, M.-H.; Yuan, D.-Q.; Fang, Q.-R.; Li, J.-R.; Ribas, J.; Zhou, H.-C. *Inorg. Chem.* **2010**, *49*, 769.
- (15) Liu, G. F.; Ye, B.-H.; Ling, Y.-H.; Chen, X.-M. *Chem. Commun.* **2002**, 1442.
- (16) Li, T.-H.; Lu, J.; Gao, S.-Y.; Cao, R. *Inorg. Chem. Commun.* **2007**, *10*, 551.
- (17) (a) Bhosekar, G.; Jess, I.; Naither, C. *Inorg. Chem.* **2006**, *45*, 6508. (b) Lu, W.-G.; Su, C.-Y.; Lu, T.-B.; Jiang, L.; Chen, J.-M. *J. Am. Chem. Soc.* **2006**, *128*, 34.